

# Polymer Chemistry

Accepted Manuscript



This is an *Accepted Manuscript*, which has been through the Royal Society of Chemistry peer review process and has been accepted for publication.

*Accepted Manuscripts* are published online shortly after acceptance, before technical editing, formatting and proof reading. Using this free service, authors can make their results available to the community, in citable form, before we publish the edited article. We will replace this *Accepted Manuscript* with the edited and formatted *Advance Article* as soon as it is available.

You can find more information about *Accepted Manuscripts* in the [Information for Authors](#).

Please note that technical editing may introduce minor changes to the text and/or graphics, which may alter content. The journal's standard [Terms & Conditions](#) and the [Ethical guidelines](#) still apply. In no event shall the Royal Society of Chemistry be held responsible for any errors or omissions in this *Accepted Manuscript* or any consequences arising from the use of any information it contains.

# A novel stimuli-responsive fluorescent elastomer based on AIE mechanism

Weili Li<sup>‡a,b\*</sup>, Dong Huang<sup>‡a</sup>, Jun Wang<sup>a</sup>, Wenjun Shen<sup>a</sup>, Lizhuang Chen<sup>a</sup>, Shengyuan Yang<sup>b</sup>,  
Meifang Zhu<sup>b</sup>, Benzong Tang<sup>c,d\*</sup>, Guodong Liang<sup>e</sup>, Zhexiao Xu<sup>f</sup>

<sup>a</sup> School of Material Science and Engineering, Jiangsu University of Science and Technology, Zhenjiang  
212003, China

<sup>b</sup> State Key Laboratory for Modification of Chemical Fibers and Polymer Materials, Donghua University

<sup>c</sup> HKUST-Shenzhen Research Institute, No. 9 Yuexing 1st RD, South Area, Hi-tech Park, Nanshan, Shenzhen  
518057, China

<sup>d</sup> Department of Chemistry, Institute for Advanced Study, Institute of Molecular Functional Materials,  
Division of Biomedical Engineering, Division of Life Science and State Key Laboratory of Molecular  
Neuroscience, The Hong Kong University of Science & Technology (HKUST), Clear Water Bay, Kowloon,  
Hong Kong.

<sup>e</sup> DSAP lab, PCFM lab, GDHPPC lab, School of Chemistry and Chemical Engineering, Sun Yat-Sen  
University, Guangzhou 510275, China.

<sup>f</sup> Suzhou Jiren Hi-Tech Material Co., Ltd, Suzhou 215143.

<sup>‡</sup> These authors contributed equally to this work.

34 **Abstract:** In this paper, a facile approach for the synthesis of stimuli-responsive  
35 fluorescent elastomer was developed. Tetraphenylethylene (TPE) derivant was linked to  
36 flexible polydimethylsiloxane(PDMS) polymer chains by covalent-bond with silane  
37 coupling agent, followed by condensation reaction with tetraethylorthosilicate(TEOS) as  
38 the curing agent via sol-gel reaction to obtain the fluorescent elastomer. <sup>1</sup>HNMR and FTIR  
39 spectroscopy studies showed the degree of the reaction, and the homogeneous distribution  
40 of TPE derivant in the elastomer was confirmed by SEM, XRD and PL spectra, respectively.  
41 Due to the hampered intramolecular rotation of the aryl rotors of dye molecules with the  
42 intertwined polymer chains, the cured elastomers showed intense fluorescent emission. In  
43 addition, the elastomers exhibited stimuli-sensitive fluorescence against temperature, and  
44 its responsiveness was found to be reversible.

## 45 **Introduction**

46 With the progress of the times, new requirements are presented to the people. The  
47 development of modern technologies requires the materials combination of properties that  
48 cannot be provided by just ordinary polymers. Moreover, the continuous interest on the  
49 commonly called smart materials has also been extremely stimulated by the recent  
50 European Council regulation on plastic packages that is under revision to include active  
51 and intelligent systems, the latter being able to constantly monitor the quality of the  
52 packaged material during transport and storage<sup>[1-4]</sup>. Fluorescent organic molecules have  
53 been vigorously investigated due to the interesting photophysical properties accompanied  
54 by their intrinsic softness and lightness. Many researches have focused on their  
55 applications for such as organic light-emitting diodes (OLED), semiconductor laser, and  
56 fluorescent sensors<sup>[5-7]</sup>. In general, they present prominent fluorescence in a solution, not  
57 in a solid state due to aggregation-caused quenching (ACQ) phenomenon, while the  
58 practical uses of them are based on their solid state such as film<sup>[8-9]</sup>. However, fundamental  
59 molecular design of organic molecules exhibiting highly efficient solid-state luminescence  
60 is still ambiguous.

61 In 2001, a novel phenomenon of aggregation-induced emission(AIE) was first found  
62 by Tang's group from propeller-like siloles, whose emission was very weak in solution but

63 became intense as aggregates formed<sup>[10]</sup>. Such abnormal emission behavior has drawn  
64 great research interest, for it is exactly opposite to the common belief that the emission of  
65 chromophores decreases in the aggregate state<sup>[11-13]</sup>. This intriguing finding paves a new  
66 avenue to tackle the notorious ACQ of conventional chromophores. Tetraphenylethene  
67 (TPE) is one of the typical fluorescent molecule with AIE character, and it is found to be  
68 non-emissive in dilute solutions but became highly luminescent when their molecules are  
69 aggregated in concentrated solutions or cast in solid films<sup>[14]</sup>. In detail, in a dilute solution,  
70 TPE undergoes dynamic intramolecular rotations against its double bond and renders its  
71 molecule non-luminescent. On the other hand, in the aggregate state, the molecules cannot  
72 pack through a  $\pi$ - $\pi$  stacking process due to its propeller shape, while the intramolecular  
73 rotations of its aryl rotors are greatly restricted owing to the physical constraint. This  
74 restriction blocks the non-radiative pathway and opens up the radiative channel<sup>[15-16]</sup>.

75 With rapid extension of the application of fluorescent materials, including biological  
76 monitoring, lithography, solar cells and selective membranes, it is very interesting to design  
77 or modify novel AIE luminogens to make them into application<sup>[17]</sup>. Xiqi Zhang et al  
78 synthesized piezofluorochromic aggregation-induced emission (PAIE) materials which  
79 possessed both piezofluorochromic and aggregation-induced emission properties<sup>[18]</sup>. Zujin  
80 Zhao et al synthesized novel 1,3,6,8-tetrakis [4-(1,2,2-triphenylvinyl) phenyl] pyrene  
81 (TTPEPy) with a novel AIEE effect, efficient solid PL ( $\Phi_F = 70\%$ ), and excellent thermal  
82 stability ( $T_d = 485^\circ\text{C}$ ). The AIEE effect enables TTPEPy to work as a solid emitter for the  
83 construction of efficient OLEDs, with  $\eta_C$ ,  $\eta_P$  and  $\eta_{\text{ext}}$  up to  $12.3 \text{ cd A}^{-1}$ ,  $7.5 \text{ lm W}^{-1}$  and  
84  $4.95\%$ , respectively<sup>[19]</sup>. Xiqi Zhang et al provided tetraphenylethene-based AIE FONs  
85 (TPE-Ply), with facile preparation procedure, AIE property, uniform morphology, high  
86 water dispersibility and excellent biocompatibility, they were expected to be novel and  
87 promising for cell imaging applications<sup>[20]</sup>.

88 Taking the advantage of AIE luminogens, the fluorescence intensity of the modified  
89 polymers can be efficiently enhanced by increasing its concentration, loading without the  
90 need to avoid the aggregation of the probes. However, it is strongly necessary to figure out  
91 how the AIE luminogens and the polymer will interact with each other, and how the

92 interaction will impact on the products' fluorescence properties.

93 In this paper, we synthesized TPE derivant and knitted it to PDMS polymer chains  
94 by covalent bonds to study its fluorescence property. PDMS based elastomer is known to be  
95 rubbery material consisting of soft and flexible polymer chains with cross-linking points;  
96 thus the movement of the polymer chains seriously affect the degree of bondage to AIE  
97 luminogen. Importantly, the application of AIE luminogen functionalized elastomer may  
98 not be limited to the fluorescent material, their tunable emission wavelength and good  
99 stimuli-sensitive fluorescence properties may make them to be applied into thermal  
100 detection and so on.

## 101 **Results and discussion**

102 Compound TPE-containing dibenzyl bromide (TPE-2CH<sub>2</sub>Br) and its synthetic  
103 process are presented in Scheme 1 and Scheme 2, respectively. Detailed procedures can be  
104 found in the supporting information.

105 -----**Scheme 1**-----

106 TPE-2CH<sub>2</sub>Br was then knitted to PDMS polymer chains by covalent bond with  
107 APTES. The synthetic process is presented as follows (Scheme 3). Detailed procedures can  
108 be found in the supporting information. To study the influence of AIE luminogen content  
109 on the properties of the elastomers, the weight ratio of TPE-2CH<sub>2</sub>Br to PDMS varied from  
110 1:10<sup>-2</sup> to 1:10<sup>-4</sup> as presented in Table 1, and the corresponding oligomer were named as  
111 TPE-PDMS-A, TPE-PDMS-B, TPE-PDMS-C, TPE-PDMS-D, and TPE-PDMS-E,  
112 respectively.

113 -----**Scheme 2**-----

114 -----**Scheme 3**-----

115 -----**Table 1**-----

116 Then, TPE-PDMS fluorescent elastomers were prepared by sol-gel reaction. At first,  
117 TPE-PDMS oligomers were blended with TEOS at weight ratio of 100:30; after being  
118 added into DBTDL(0.05wt%), the blends were casted onto the substrate. The fluorescent  
119 elastomers were got by being heated at 80°C for 8h. To identity clearly, the solidified  
120 fluorescent elastomers were named as STP-A, STP-B, STP-C, STP-D and STP-E,

121 respectively. Because TPE molecular was knitted with PDMS chains by covalent-bond, its  
122 intramolecular rotations would be restricted with the surrounding polymer chains, and the  
123 elastomer showed a typical Aggregation Induced Emission character.

124 Fig.1S shows FTIR spectra of PDMS modified with APTES and TPE-PDMS-A,  
125 respectively. The peaks at  $3750\text{cm}^{-1}$ ,  $2962\text{cm}^{-1}$  and  $1100\sim 1002\text{cm}^{-1}$  assign to  $\nu_{\text{N-H}}$ ,  $\nu_{\text{C-H}}$  and  
126  $\nu_{\text{Si-O}}$ , respectively. From these two spectra, the relative intensity absorption of N-H  
127 weakened obviously for TPE-PDMS-A because  $-\text{NH}_2$  group had been consumed during the  
128 reaction when TPE- $2\text{CH}_2\text{Br}$  was added. In addition,  $7.260(\text{m}, \text{H-Benzene})$  attributes to the  
129 benzene ring of TPE is observed from  $^1\text{HNMR}$  of TPE-PDMS-A(Fig.2S)(  $\text{CDCl}_3$  is used as  
130 the solution). These data indicate that the reaction has successfully proceeded without  
131 damaging the structures.

132 Table 1S summarizes Molecular Weight and Molecular Weight Distribution of  
133 TPE-PDMS oligomer. The cross-linking density of TPE-PDMS oligomer increased with  
134 the content of silane coupling agent because more content of PDMS was linked with each  
135 other during the reaction. The performance of the cured elastomer would be interfered by  
136 highly crosslinked PDMS oligomers. The result of GPC demonstrated this trend.

137 X-ray diffractometry (XRD) was used to characterize the dispersion of AIE  
138 luminogen in the fluorescent elastomer. No diffraction peaks from TPE- $2\text{CH}_2\text{Br}$  were  
139 detected for STP-A elastomer, suggesting that TPE- $2\text{CH}_2\text{Br}$  was uniformly dispersed in the  
140 elastomer without the formation of large aggregates probably due to its connection onto  
141 PDMS polymer chains with covalent bonds<sup>[21]</sup>.

142 -----**Fig.1**-----

143 -----**Fig.2**-----

144 Typical SEM image of the surface of STP-A elastomer, as is shown in Fig.2,  
145 conformed the conclusion of XRD. TPE- $2\text{CH}_2\text{Br}$  was uniformly dispersed in the PDMS  
146 matrix without the formation of large aggregates. A slight wrinkle might be caused by the  
147 shrinkage of polymer chains during the process of sol-gel reaction<sup>[22]</sup>.

148 Due to high chemical-bond energy ( $\text{Si-O-Si}$ ,  $422.5\text{kJ/mol}$ ), it needs more energy to  
149 destruct PDMS-based elastomer<sup>[23]</sup>. From Fig.3, pure PDMS-based elastomer showed a

150 good heat resistant property, and the thermal decomposition temperature reached 472°C.  
151 When TPE-2CH<sub>2</sub>Br is knitted to PDMS chains by covalent bonds, thermal stability of  
152 elastomer may be influenced by its lower chemical-bond energy. However, from the result  
153 of TGA, the heat resistant of STP-A could still be as high as 452°C. With the protection of  
154 the packed long polymer chains, thermal stability of AIE luminogen is enhanced effectively,  
155 which means that the cured fluorescent elastomer can still work at high temperature.

156 -----**Fig.3**-----

157 To obtain a deep insight of cross-linking in these fluorescent elastomers, differential  
158 scanning calorimetry (DSC) and dynamic mechanical analysis (DMA) were carried out on  
159 pure PDMS-based elastomer and the fluorescent elastomers, respectively. In the literature, a  
160 DSC chart of STP-X and pure PDMS-based elastomer showed one melting point at around  
161 -45°C. By increasing the crosslink density of the fluorescent elastomers, more energy is  
162 needed to destroy the crystalline lamellae due to higher molecular weight of the elastomer,  
163 so the enthalpy of the fluorescent elastomers are increased(Seen from Table 2S). These data,  
164 substantially different from those of the starting polymers, also supported the successful  
165 process of cross-linking reaction, resulting in appropriate anchoring of the employed  
166 polymer chains<sup>[24]</sup>. In addition, the result of thermodynamics measurement conformed that  
167 the mobility of the polymer chains enhanced linearly to the increased temperature above  
168 room temperature. Due to the restricting effect of the polymer chains weakens with the  
169 increased temperature, the mobility of TPE molecular increases and a part of TPE  
170 molecular can return to ground state through non-radiative way, and the intensity of  
171 photoluminescence will weaken correspondingly<sup>[25]</sup>.

172 -----**Fig.4**-----

173 -----**Fig.5**-----

174 Unlike DSC, DMA measurement provides a better accuracy of thermal phase  
175 transition readings, and more importantly, are capable of isolating the storage and loss  
176 moduli. As was demonstrated by Hill and Kozlowski<sup>[26]</sup>, the dynamic measurements are  
177 advantageous since it is possible to simultaneously measure storage and loss moduli in a  
178 rubbery plateau region. Take STP-A as an example, from its DMA curve(Fig.6), lineally  
179 decreased storage modulus meant that the motion capability of the polymer chains

180 increased linearly with the temperature and no phase transition happened during the range  
181 of testing temperature. The result of DMA is consistent with DSC, so a part of TPE  
182 molecular linked with PDMS polymer chains can return to ground state through  
183 non-radiative way, and the photoluminescence intensity of the fluorescent will weaken  
184 correspondingly.

185 -----**Fig.6**-----

186 The elucidation for mechanical properties of the fluorescent elastomers, including  
187 Strain-stress curve and Young's modulus (E), was conducted by tension experiment at room  
188 temperature. For the test, we prepared a dumbbell-like shaped specimen. From stress-strain  
189 curves, higher elongation at break and tensile strength can be obtained by more content of  
190 silane coupling agent. As we know, with longer bond length and higher bond angle, PDMS  
191 polymer chains present very soft property, PDMS-based elastomer can't be applied into  
192 application only when the polymer chains is cross-linked by covalent bonds. From the  
193 result of Stress-strain curves, STP-A presented the best elongation at break property. Firstly,  
194 the increased molecular weight and the restricted movement of polymer chains can be  
195 obtained by higher cross-linking density, which is beneficial to the mechanical properties of  
196 the fluorescent elastomer. Secondly, the knitted AIE luminogen can also act as a rigid  
197 cross-linker to the fluorescent elastomers. Young's moduli were assessed from the curves  
198 between 0.479 and 0.878 of strain (Table S3). As to STP-A, when the content of silane  
199 coupling agent was the highest, the degree of cross-linking might be best to make the  
200 polymer chains be connected at a certain degree to resist on the external forces well. In  
201 addition, the elastomer didn't present brittleness property at this stage. So the enhancement  
202 of both stress and strain maxima was observed. For pure PDMS-TEOS elastomer, it might  
203 present more like a gel. The fluorescent elastomers could offset the external force by the  
204 motion of chain segment. So it exhibited longer elongation at break and lower Young's  
205 modulus than STP-E. These values are in good agreement with those of the reported PDMS  
206 elastomers<sup>[27]</sup>.

207 Next, photophysical properties of different fluorescent oligomers and elastomers will  
208 be studied systematically. Owing to the electronic transition of the TPE unit, the absorption  
209 spectra of TPE and TPE-PDMS oligomer in diluted THF solutions (10 $\mu$ M) exhibited the



210 absorption peak at 315nm.

211 Photoluminescence (PL) spectra of TPE-PDMS oligomers present a strongly  
212 fluorescent property, and concentration dependent increase of intensity. We have proposed  
213 that restriction of intramolecular rotation (RIR) is the main cause for the AIE phenomenon  
214 [28]. When TPE devriant and polymer chains were knitted together by covalent bonds, the  
215 RIR process would partially activate and thus make the oligomer&elastomer somewhat  
216 emissive. According to Fig.7, the intensity of PL spectra increased linearly to the  
217 concentration of TPE devriant. With the connection effect of covalent bonds and similar  
218 chemical environment, the intensity of PL spectra didn't present an abrupt change. These  
219 data demonstrated that TPE devriant homogeneously dispersed in the elastomeric samples  
220 without forming macroscopic aggregates or domains.

221 -----Fig.7-----

222 In addition, a slight red shift was observed from TPE-PDMS-E(475nm) to  
223 TPE-PDMS-A(491nm). It might be caused by the intramolecular charge transfer (ICT)<sup>[29-31]</sup>  
224 mechanism. Although TPE-2CH<sub>2</sub>Br was linked to PDMS polymer chains by covalent  
225 bonds, the modified PDMS can also act as "solid-state solvent" to the AIE luminogen. With  
226 more silane coupling agent in the elastomer, higher polarity of the surrounding "solid-state  
227 solvent" will lead to a slight red-shift of the emission maximum. In the next, TPE-PDMS-A  
228 oligomer and STP-A elastomer were taken as examples because they showed the most  
229 obvious fluorescence behavior.

230 To identify the difference between TPE devriant and TPE-PDMS-A oligomer in  
231 photoluminescence performance, we examined the emission behaviors of TPE-2CH<sub>2</sub>Br and  
232 TPE-PDMS-A in THF and THF-water mixtures. The PL spectrum of TPE-2CH<sub>2</sub>Br in THF  
233 was basically a flat line parallel to the abscissa (Fig.8A). However, when a large amount of  
234 water ( $\geq 90$  vol%) was added to THF solution, an emission peak emerged at 468 nm, the PL  
235 intensity was 31-fold higher than that of pure THF solution, demonstrating a typical  
236 AIE(Aggregation-Induced Emission) phenomenon<sup>[32,33]</sup>. For TPE-PDMS oligomer, on the  
237 other hand, it behaved differently. TPE-PDMS-A showed apparent fluorescent in THF  
238 solution, and the emission peak emerged at 490nm (Fig.8B). When a small amount of water  
239 was added into THF solution, obvious fluorescence enhancement was observed. The

240 emission became stronger progressively with increasing the amount of water in the solvent  
241 mixture. At 90 vol% water content, the PL intensity was 3.3-fold higher than that of pure  
242 THF solution, while the emission maximum was still located at 490nm. It presented a  
243 typical AEE(Aggregation-Enhanced Emission). The changes in the relative PL intensity  
244 ( $I/I_0$ ) with the solvent composition of THF-water mixtures of TPE-2CH<sub>2</sub>Br and  
245 TPE-PDMS-A oligomer are given in Fig.9.

246 -----Fig.8-----

247 -----Fig.9-----

248 While the PL intensity of TPE-2CH<sub>2</sub>Br solution rose abruptly after threshold water  
249 content, a smooth emission enhancement with the water content was observed in  
250 TPE-PDMS-A. Being a low molecular weight compound, the molecule of TPE-2CH<sub>2</sub>Br is  
251 free to rotate in pure THF solution as well as THF-water mixtures with low water contents.  
252 In contrast, TPE-2CH<sub>2</sub>Br and PDMS polymer chains in TPE-PDMS oligomers are knitted  
253 together, which partially activate the RIR process and thus make the polymer somewhat  
254 emissive even in pure THF solution. Moreover, due to higher hydrophobicity or  
255 comparatively low solubility of TPE-PDMS in aqueous mixture, aggregates are more  
256 readily formed in THF-water mixtures with low water fractions, thus making the PL  
257 process of the polymer more sensitive to the change in its surrounding solvent medium<sup>[25,34]</sup>.  
258 In addition, the slight red-shift of the emission maximum (from ~468 to 490 nm) when TPE  
259 derivant was linked to PDMS polymer chains might be also caused by ICT mechanism and  
260 the reason had been discussed as above.

261 Interaction between PDMS and TPE-2CH<sub>2</sub>Br can also impact on the photophysical  
262 property of the fluorescent oligomer&elastomer. As presented in Fig.10(A), when TPE  
263 derivant was physical blended with PDMS oligomer in THF solution, no fluorescence  
264 could be observed. On the contrary, TPE-PDMS oligomer, which TPE derivant was knitted  
265 with PDMS polymer chains via covalent bond, could show obvious fluorescence in THF  
266 solution. As to the former blending solution, AIE luminogen is free to rotate in polymer  
267 solution, so the absorbed energy can be released through a non-radiative pathway. However,  
268 when intramolecular rotation of TPE derivant are restricted by the knitted polymer chains,  
269 the RIR process would activate and make TPE-PDMS oligomers emissive in pure THF

270 solution. The fluorescent elastomer STP-A, as presented in Fig.10(B), showed similar  
271 behavior. The STP-A elastomer displayed intensive fluorescence while the cured PDMS  
272 elastomer blended with TPE-2CH<sub>2</sub>Br could only show extremely weak fluorescence. With  
273 good miscibility between PDMS and TPE derivant, TPE-2CH<sub>2</sub>Br was uniformly dispersed  
274 in PDMS matrix without the formation of large aggregates. The reason for weak  
275 fluorescence intensity may be caused by low concentration of TPE-2CH<sub>2</sub>Br in the system at  
276 first. In addition, the flexibility of the PDMS polymer chains should also be taken into  
277 account. In this state, there are no covalent links between PDMS polymer chains and AIE  
278 luminogen. TPE undergoes dynamic intramolecular rotations against its double bond and  
279 renders its molecule non-luminescent because there is no bondage action to it.

280 -----**Fig.10**-----

281 In addition, a slight red-shift of the emission maximum for the fluorescent elastomers  
282 (from ~490 to 500 nm) might be also caused by the ICT mechanism as was discussed  
283 above: the joint hydrolysed-TEOS will enhance the polarity of the cured elastomer<sup>[35,36]</sup>.

284 -----**Fig.11**-----

285 PL spectra and PL intensity of STP-A varied with temperatures and are presented in  
286 Fig.11(A) and (B), respectively. The result verified the conjecture of the results of DSC and  
287 DMA. The fluorescent elastomer emitted a strong green-blue light (500 nm) at room  
288 temperature. With the raised temperature, the fluorescence intensity of the fluorescent  
289 elastomer decreased. Because TPE molecules are embedded in the polymer matrices and  
290 knitted with each other, the intramolecular motions (i.e. rotation, vibration, torsion, and  
291 bending) of the phenyl rings of TPE are restricted to some extent. The energy of the excited  
292 state is annihilated through radiation decay, and thus AIE luminogen emits efficiently.  
293 Because there was no transition temperature determined in the temperature range 0°C  
294 ~150°C, segmental motion capability increased linearly with the increased temperature.  
295 Plots of fluorescence intensity at 500 nm against temperature showed that the fluorescence  
296 intensity dropped linearly and drastically with the increased temperature. The  
297 intramolecular motions consume the energy of the excited state, which leads to weak  
298 fluorescence emission of AIE luminogen in the rubbery state of the polymers<sup>[37,38]</sup>.

299 -----**Fig.12**-----

300 To study the durability of the fluorescent elastomer, STP-A was selected and checked  
301 at various temperatures. From Fig.12, STP-A elastomer showed similar fluorescence image  
302 between 30°C and 150°C. The fluorescence spectra of STP-A at 30°C showed a distinct  
303 emission peak at 500nm, whereas the emission was considerably weaker at 150°C. The  
304 fluorescence emission was capable of reversibly switching by repeatedly altering  
305 temperature. This revealed that STP-A was stable for repeated thermal treatments.

## 306 **Conclusions**

307 In summary, we demonstrated a synthesis of fluorescent elastomer by knitting  
308 TPE-2CH<sub>2</sub>Br with PDMS together via covalent bonds. Facile progress of the preparative  
309 reaction was confirmed by <sup>1</sup>HNMR and FTIR spectroscopy studies. The copolymerized  
310 TPE derivant didn't ruin the heat resistance of the cured fluorescent elastomer as could be  
311 confirmed by TGA; in addition, it is uniformly dispersed in the elastomer without the  
312 formation of large aggregates from the overall results of SEM, XRD and PL spectroscopy.  
313 A tensile test of the obtained sample strips showed archetypal elastomeric behavior, while  
314 the content of silane coupling agent and AIE luminogen substantially affected on their  
315 mechanical properties such as Young's modulus and maximum strain. Fluorescence of the  
316 oligomer and the cured elastomers were found to be affected by the interaction between  
317 PDMS polymer chains and TPE-2CH<sub>2</sub>Br, only when they were knitted together with  
318 covalent bond, could activate the RIR process and make the elastomer somewhat emissive.  
319 It should partly be attributed to the hampered intramolecular rotation of the aryl rotors of  
320 dye molecules by wrapping and coiling of flexible polymer chains. Fluorescence of the  
321 elastomers was found to be stimuli-sensitive against temperature, and reversibility of this  
322 responsiveness was also confirmed. The AIE characteristics are clearly responsible for  
323 these features, which is also susceptible for the RIR process. With significant advantages,  
324 such as ease of synthesis, high and tunable sensitivity, immunity to aggregation, facile  
325 operation and data processing, TPEs offer new opportunities for combination of AIE  
326 luminogen into elastomeric polymer network to open a new horizon for material chemistry,  
327 such as sensing materials for temperature and so on.

## 328 **Experimental**

**329 Materials**

330 PDMS( $M_w=1.3\times 10^5$ ) was purchased from Jinan Beyond Co.,Ltd., China.  
331 Tetrahydrofuran (THF) was distilled under normal pressure from sodium benzophenone  
332 ketyl under nitrogen. Aminopropyltriethoxysilane(APTES), 4-bromobenzophenone, zinc  
333 powder, titanium (IV) chloride ( $TiCl_4$ ), tetraethoxysilane(TEOS), dibutyltin dilaurate  
334 (DBTDL) and other chemicals and solvents were all purchased from Aldrich and used as  
335 received without further purification.

**336 Instruments**

337  $^1H$ NMR spectra were measured on Bruker ARX 400 NMR spectrometers using  $CDCl_3$   
338 as the deuterated solvent and tetramethylsilane (TMS;  $\delta=0$ ppm) as the internal standard.  
339 FTIR spectra were recorded on a Perkin-Elmer 16 PC FT-IR spectrophotometer. Relative  
340 number ( $M_n$ ) and weight-average ( $M_w$ ) molecular weights and polydispersity indices (PDI  
341 or  $M_w/M_n$ ) of the TPE-PDMS oligomers were estimated by a Waters Associates gel  
342 permeation chromatography (GPC) system equipped with RI and UV detectors. THF was  
343 used as the eluent at a flow rate of  $1.0\text{ mL min}^{-1}$ . A set of monodispersed linear  
344 polystyrenes covering the molecular weight range of  $10^3\sim 10^7$  was used as the standard for  
345 the molecular weight calibration. X-ray diffraction (XRD) measurements were performed  
346 using an XRD diffractometer(D-MAX 2200 VPC) equipped with Ni-filtered Cu  $K\alpha$   
347 radiation, having a wavelength of 0.154nm. Images of scanning electron microscopy were  
348 taken on a JSM-6700F electron microscope. Thermogravimetric analysis (TGA)  
349 measurements were carried out under nitrogen or in air on a Perkin-Elmer TGA 7 analyzer  
350 at a heating rate of  $10^\circ\text{C min}^{-1}$ . DSC measurements were carried out using DSC Q100 (TA  
351 Instruments) (TA Instruments, USA) over the temperature of  $-80^\circ\text{C}$  to  $200^\circ\text{C}$  at a scan rate  
352 of  $10^\circ\text{C min}^{-1}$ . All the thermograms were base line corrected and calibrated using Indium  
353 metal. The experimental specimens (8–10 mg) were dried at  $60^\circ\text{C}$  under vacuum for 24h,  
354 before being measured. All the samples were firstly annealed at  $120^\circ\text{C}$  for 3 min, and  
355 cooled to  $-80^\circ\text{C}$  by using liquid nitrogen and then scanned for the measurement. Tensile  
356 properties of were measured through a 10 kN electromechanical tensile testing machine  
357 (CMT5104, China) at room temperature, and the tensile speed was  $50\text{ mm min}^{-1}$ . UV-vis  
358 absorption and light transmission spectra were measured on a Milton Roy Spectronic 3000

359 array spectrophotometer. Dynamic mechanical analysis (DMA) was done by DMA242,  
360 (NETZSCH, Germany) measurement. It was carried on from room temperature to 150°C at a  
361 scan rate of 10°C min<sup>-1</sup>, with 80µm amplitude of vibration and 1Hz frequency of the  
362 alternating stress. Fluorescence spectra were recorded using a steady state spectrometer  
363 (Edinburgh Instrument Ltd, FLSP920) equipped with a temperature control system (Oxford  
364 instruments). To eliminate the interference of heating rates on the thermal properties of the  
365 fluorescent elastomer, heating rate was fixed at 1 min<sup>-1</sup> for all specimens. Fluorescence  
366 spectra were scanned every 1 min.

### 367 **Acknowledgements**

368 The project was funded by State Key Laboratory for Modification of Chemical  
369 Fibers and Polymer Materials, Donghua University, NSFC (No.21201087), Postdoctoral  
370 Foundation of Jiangsu Province (NO.1501091c), and  
371 National Natural Science Foundation of China (No. 21201087). Author also thanks Jiangsu  
372 Overseas Research & Training Program for University Prominent Young & Middle-aged  
373 Teacher and Presidents, and the Innovative Programs for Undergraduate Students of and  
374 Innovative Programs for Graduate Students of Jiangsu University of Science and  
375 Technology.

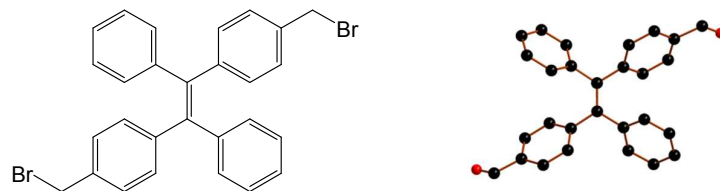
### 376 **Notes and references**

- 377 1. A. Pucci, G. Ruggeri, *J. Mater. Chem.*, 2001, **21**, 8282-8291.
- 378 2. A. Pucci, G. Bizzarri and G. Ruggeri, *Soft Mater.*, 2011, **7**, 3689-3700.
- 379 3. C. Weder, *J. Mater. Chem.*, 2011, **21**, 8235-8236.
- 380 4. D. A. Davis, A. Hamilton, J. L. Yang, L. D. Cremer, D. Van Gough, S. L. Potisek, M. T. Ong, P. V. Braun,  
381 T. J. Martinez, S. R. White, J. S. More and N. R. Sottos, *Nature*, 2009, **459**, 68-72.
- 382 5. R. H. Friend, R.W. Gymer, A. B. Holmes, J. H. Burroughes, R. N. Marks, C. Taliani, D.D.C. Bradley, D.  
383 A. Dos Santos, J. L. Brédas, M. Lögdlund and W.R. Salaneck, *Nature*, 1999, **397**, 121-128.
- 384 6. I. D. W. Samuel, G. A. Turnbull. *Chem. Rev.*, 2007, **107**, 1272-1295.
- 385 7. S. W. Thomas, G. D. Joly and T. M. Swager. *Chem. Rev.*, 2007, **107**, 1339-1386.
- 386 8. A. Menon, M. Galvin, K. A. Walz and L. Rothberg. *Synth. Met.*, 2004, **141**, 197-202.
- 387 9. C.-T. Chen, *Chem. Mater.*, 2004, **16**, 4389-4400.

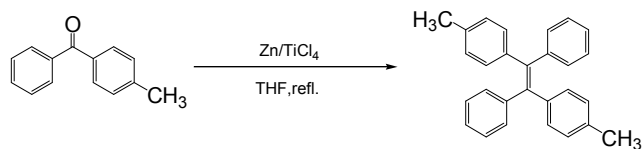
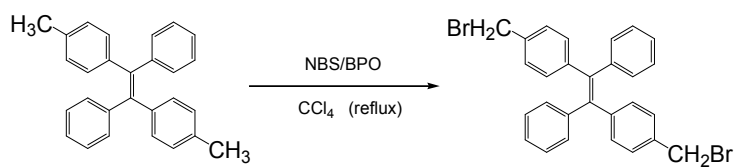
- 388 10. J. Luo, Z. Xie, J. W. Y. Lam, L. Cheng, B. Z. Tang, H. Chen, C. Qiu, H. S. Kwok, X. Zhan, Y. Liu and D.  
389 Zhu. Chem. Commun., 2001, 1740–1741.
- 390 11. Y. N. Hong, J. W. Y. Lam and B. Z. Tang, Chem. Commun., 2009, 4332–4353.
- 391 12. J. Mei, Y. N. Hong, J. W. Y. Lam, A. J. Qin, Y. H. Tang and B. Z. Tang, Adv. Mater., 2014, **26**,  
392 5429-5479.
- 393 13. R. R. Hu, Nelson L. C. Leung and B. Z. Tang, Chem. Soc. Rev., 2014, **43**, 4494-4562.
- 394 14. Z. F. Chang, Y. B. Jiang, B. R. He, J. Chen, Z. Y. Yang, P. Lu, H. S. Kwok, Z. J. Zhao, H. Y. Qiu and B. Z.  
395 Tang, Chem. Commun., 2013, **49**, 594-596.
- 396 15. J. Yang, N. Sun, J. Huang, Q. Q. Li, Q. Peng, X. Tang, Y. Q. Dong, D. G. Ma and Z. Li, J. Mater. Chem.  
397 C., 2015, **3**, 2624-2631.
- 398 16. J. Q. Shi, N. Chang, C. H. Li, J. Mei, C. M. Deng, X. L. Luo, Z. P. Liu, Z. S. Bo, Y. Q. Dong and B. Z.  
399 Tang, Chem. Commun., 2012, **48**, 10675-10677.
- 400 17. S. P. Bao, Q. H. Wu, W. Qin, Q. L. Yu, J. Wang, G. D. Liang and B. Z. Tang, Polym. Chem., 2015, **6**,  
401 3537-3542.
- 402 18. X. Q. Zhang, Z. G. Chi, H. Y. Li, B. J. Xu, X. F. Li, W. Zhou, S. W. Liu, Y. Zhang, and J. R. Xu, Chem.  
403 Asian J. 2011, **6**, 808-811.
- 404 19. Z. J. Zhao, S. M. Chen, Jacky W. Y. Lam, P. Lu, Y. C. Zhong, K. S. Wong, H. S. Kwok and B. Z. Tang,  
405 Chem. Commun., 2010, **46**, 2221-2223.
- 406 20. X. Q. Zhang, M. Y. Liu, B. Yang, X. Y. Zhang, Y. Wei, Colloids and Surfaces B: Biointerfaces., 2013, **112**,  
407 81-86.
- 408 21. W. L. Li, Y. M. Gao and S. M. Wang, J. Appl. Polym. Sci., 2012, **125**, 1027-1032.
- 409 22. W. L. Li, D. Huang, X. Y. Xing, J. J. Tang, Y. J. Xing, X. J. Li and J. D. Zhang, J. Appl. Polym. Sci., 2014,  
410 **131**, 41010.
- 411 23. R. Taniguchi, T. Yamada, K. Sada and K. Kokado. Macromolecules, 2014, **47**, 6382-6388.
- 412 24. R. R. Hu, Jacky W. Y. Lam, Y. Yu, Herman H. Y. Sung, Ian D. Williams, Matthew M. F. Yuen and B. Z.  
413 Tang, Polym. Chem., 2013, **4**, 95-105.
- 414 25. L. W. Hill, K. Kozlowski. J. Coat. Technol., 1987, **63**, 751-758.
- 415 26. J. Y. Wong, J. B. Leach, X. Q. Brown, Surf. Sci., 2004, **570**, 119-133.
- 416 27. Y. N. Hong, Jacky W. Y. Lam and B. Z. Tang, Chem. Soc. Rev., 2011, **40**, 5361-5388.

- 417 28. Q. S. Liu, X. Q. Wang, H. Yan, Y. P. Wu, Z. Y. Li, S. W. Gong, P. Liu and Z. P. Liu, *J. Mater. Chem. C*,  
418 2015, **3**, 2953-2959.
- 419 29. R. Hu, S. Y. Li, Y. Zeng, J. P. Chen, S. Q. Wang, Y. Li and G. Q. Yang, *Phys. Chem. Chem. Phys.*,  
420 2011, **13**, 2044-2051.
- 421 30. J. S. Wu, W. M. Liu, J. C. Ge, H. Y. Zhang and P. F. Wang, *Chem. Soc. Rev.*, 2011, **40**, 3483-3495.
- 422 31. Y. Q. Dong, Jacky W. Y. Lam, A. J. Qin, J. Z. Liu, Z. Li, and B. Z. Tang, *Applied Physics Letter* 2007, **91**,  
423 011111.
- 424 32. J. Huang, X. Yang, J. Y. Wang, C. Zhong, L. Wang, J. G. Qin and Z. Li, *J. Mater. Chem.*, 2012, **22**,  
425 2478-2484.
- 426 33. G. D. Liang, Jacky W. Y. Lam, W. Qin, J. Li, N. Xie and B. Z. Tang, *Chem. Commun.*, 2014, **50**,  
427 1725-1727
- 428 34. A. Pucci, G. Iasilli, F. Tantussi, F. Fuso and G. Ruggeri, 6<sup>th</sup> International Conference on Times of  
429 Polymers(TOP) and Composites AIP Conf. Proc., 2012, **1459**, 89-91.
- 430 35. X. Du, J. H. He, *Nanoscale*, 2011, **3**, 3984-4002.
- 431 36. B. P. Kapgate, C. Das, *RSC Adv.*, 2014, **4**, 58816-58825.
- 432 37. J. W. Chen, C. C. W. Law, J. W. Y. Lam, Y. P. Dong, S. M. F. Lo, I. D. Williams, D. B. Zhu and B. Z.  
433 Tang, *Chem. Mater.*, 2003, **15**, 1535-1546.
- 434 38. P. Y. Gu, C. J. Lu, F. L. Ye, J. F. Ge, Q. F. Xu, Z. J. Hu, N. J. Li and J. M. Lu, *Chem. Commun.*, 2012, **48**,  
435 10234-10236.

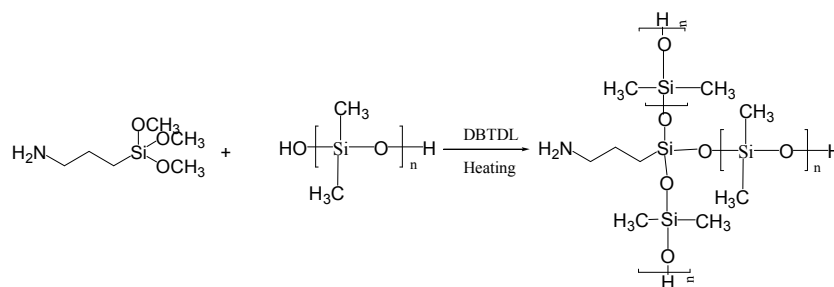




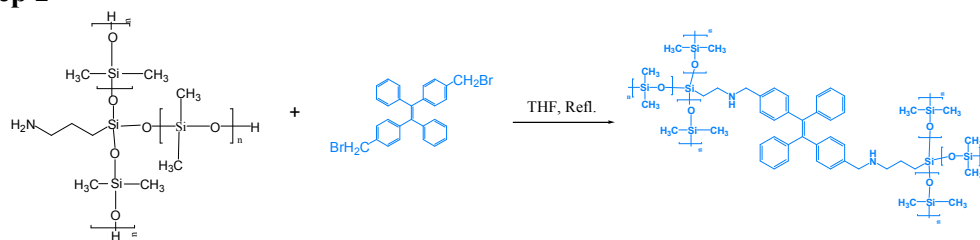
**Scheme 1.** Chemical structure and ball-rod modelling of TPE-2CH<sub>2</sub>Br

**Step 1****Step 2****Scheme 2.** Synthetic process of TPE-2CH<sub>2</sub>Br

## Step 1



## Step 2



Scheme 3. Synthetic process of TPE-PDMS oligomer

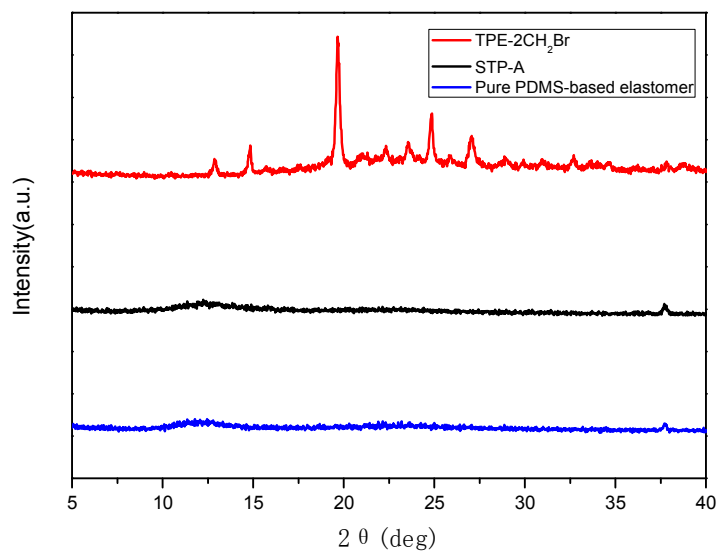


**Fig.1** XRD curves of TPE-2CH<sub>2</sub>Br, STP-A and pure PDMS-based elastomer

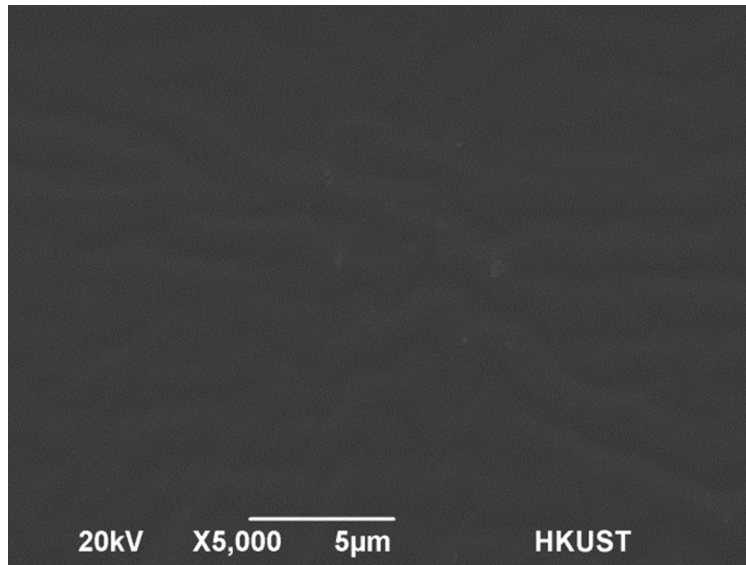


**Fig.2** SEM image of STP-A elastomer

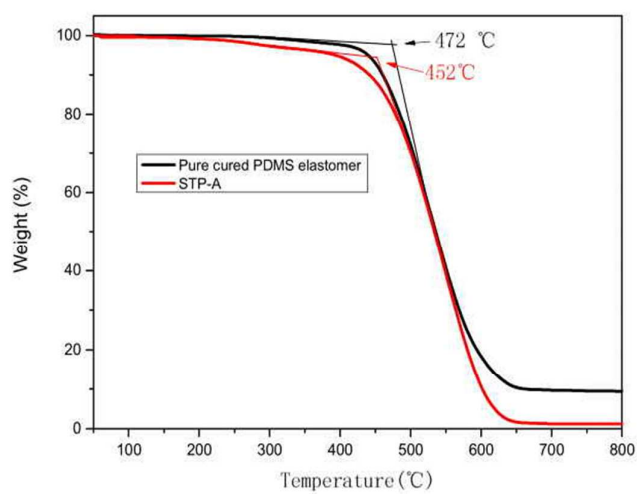


**Fig.3** Heat resistant of pure PDMS-based elastomer and STP-A elastomer

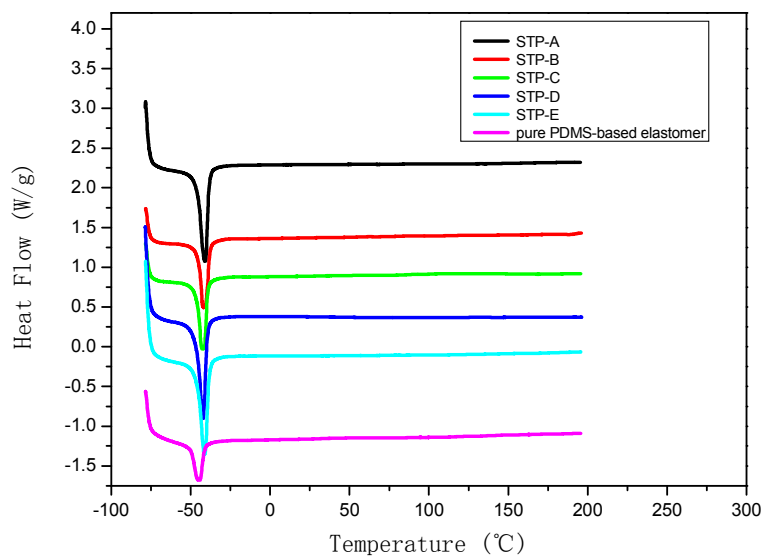


**Fig.4** DSC charts of STP-X and pure PDMS based elastomers

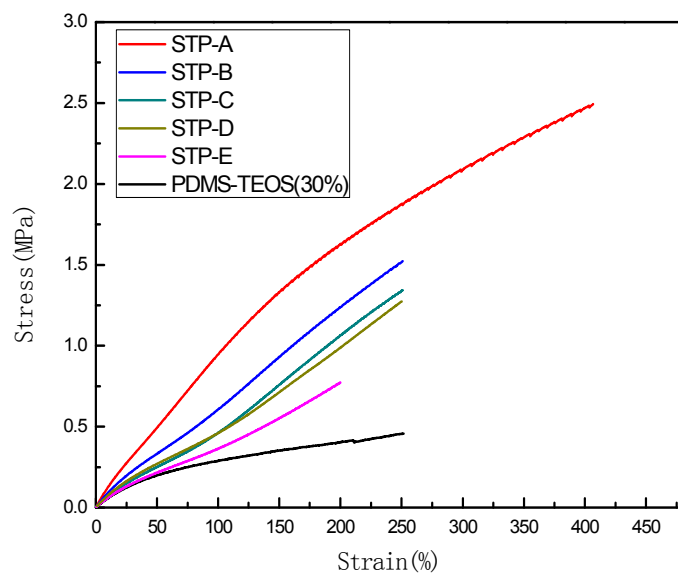


**Fig.5** Stress–strain curves measured at room temperature for different elastomers



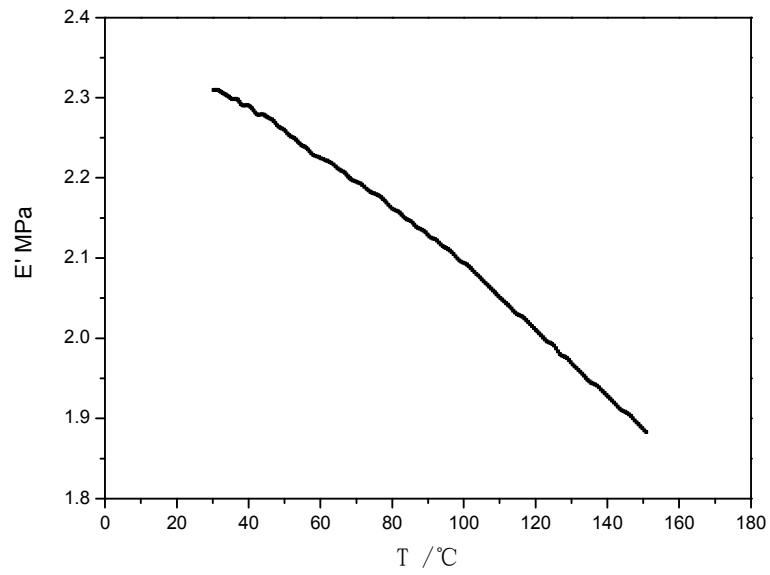


**Fig.6** DMA curve of STP-A(log  $E'$ )

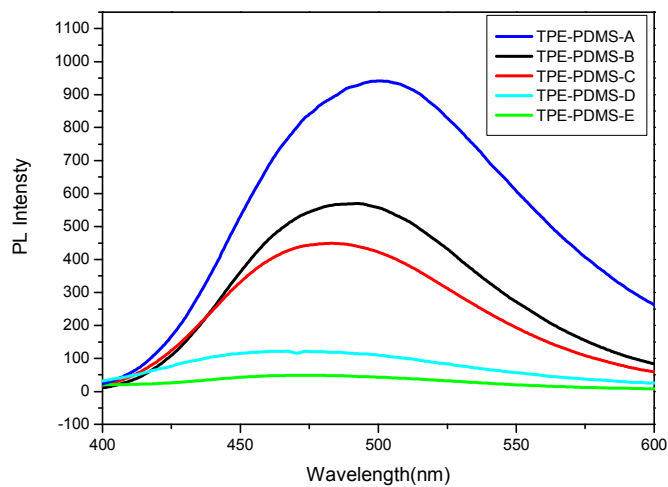


**Fig.7** PL spectra of TPE-PDMS varied with the content of TPE,  $\lambda_{\text{ex}}=315$  nm

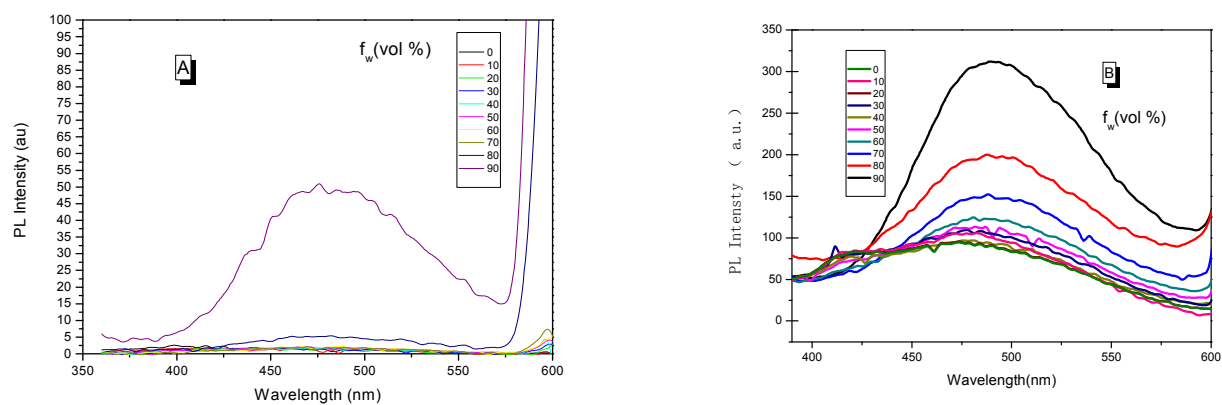


**Fig.8** PL spectra of (A) 2CH<sub>2</sub>Br-TPE and (B) TPE-PDMS-A in THF–water mixtures with different water contents ( $f_w$ ), 10 $\mu$ M,  $\lambda_{ex}$ =315 nm

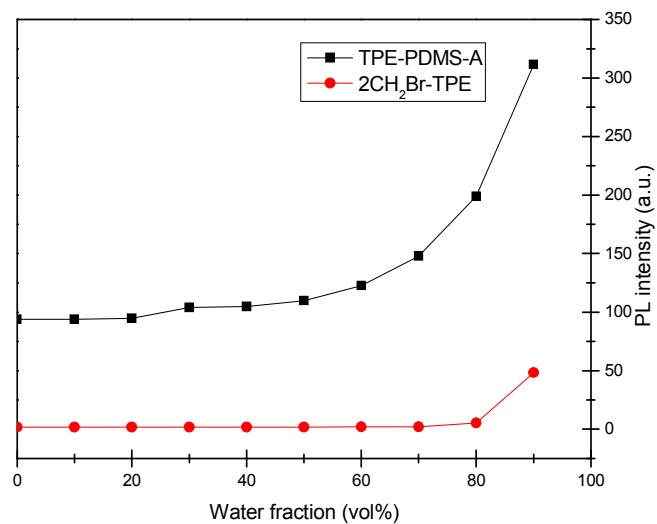


**Fig.9** PL spectra of 2CH<sub>2</sub>Br-TPE and TPE-PDMS-A in THF–water mixtures with different water contents ( $f_w$ )

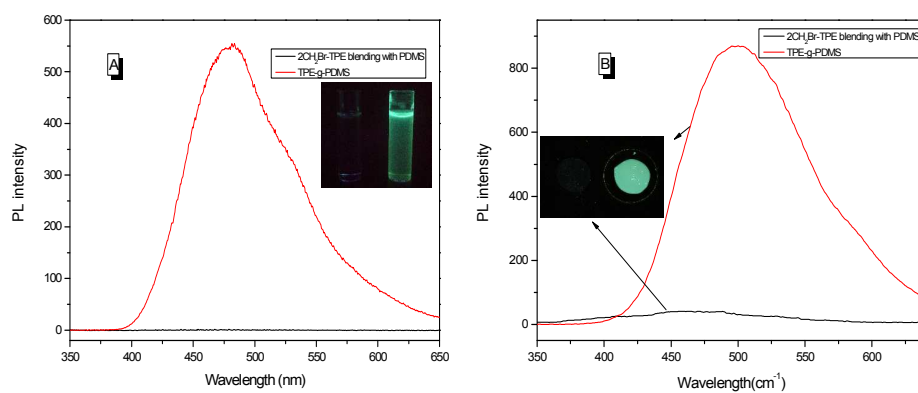


**Fig.10** (A) PL spectra of PDMS blended with TPE-2CH<sub>2</sub>Br and TPE-PDMS-A in THF solution, 10 $\mu$ M,; (B) PL spectra of the cured PDMS elastomer blended with TPE-2CH<sub>2</sub>Br and STP-A elastomer,  $\lambda_{ex}$ = 315 nm

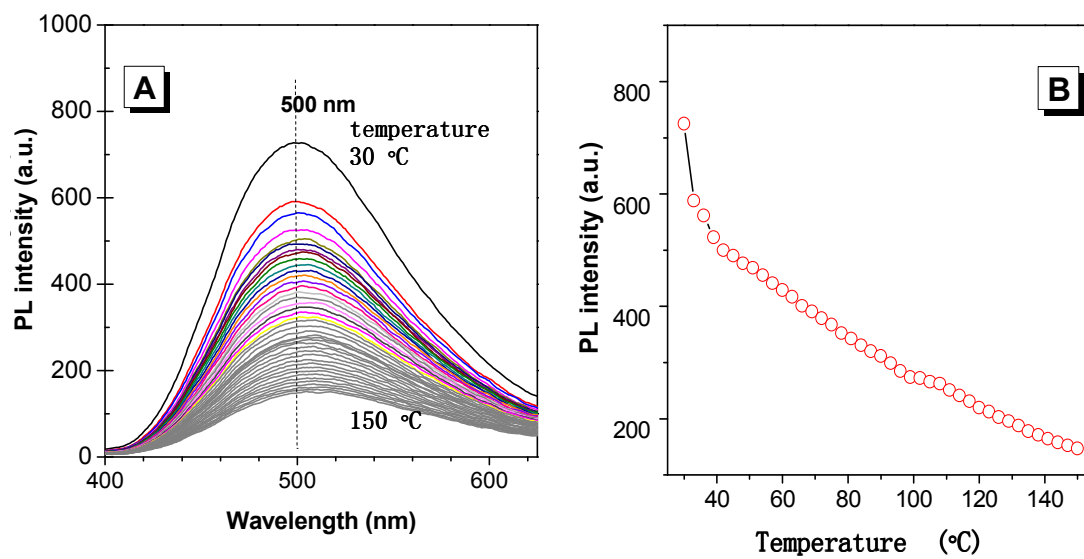


**Fig.11** (A) PL spectra of STP-A varied with temperature; (B) PL intensity varied with temperature of STP-A,  $\lambda_{\text{ex}}=315$  nm

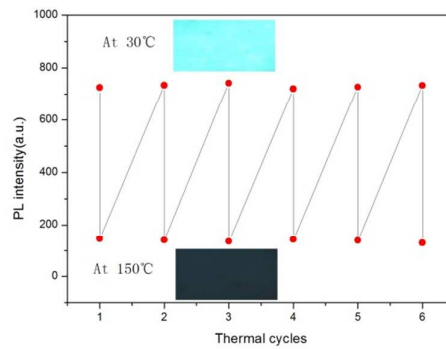


**Fig.12** Fluorescence image and its intensity (500 nm) of STP-A elastomer at 30 °C and 150 °C

**Table 1.** Preparation Condition of TPE-PDMS oligomer

<b>Materials</b>	<b>PDMS:APTES:TPE-2CH<sub>2</sub>Br *</b>
<b>TPE-PDMS-A</b>	10 <sup>2</sup> :1:1
<b>TPE-PDMS-B</b>	5×10 <sup>2</sup> :1:1
<b>TPE-PDMS-C</b>	10 <sup>3</sup> :1:1
<b>TPE-PDMS-D</b>	5×10 <sup>3</sup> :1:1
<b>TPE-PDMS-E</b>	10 <sup>4</sup> :1:1

\*By weight